Scripta Materialia 123 (2016) 135–139

Contents lists available at ScienceDirect

Scripta Materialia

journal homepage: www.elsevier.com/locate/scriptamat

Regular Article

Edge dislocations bowing out from a row of collinear obstacles in Al

Shuozhi Xu [a,*], Liming Xiong [b], Youping Chen [c], David L. McDowell [a,d]

[a] GWW School of Mechanical Engineering, Georgia Institute of Technology, Atlanta, GA 30332-0405, USA
[b] Department of Aerospace Engineering, Iowa State University, Ames, IA 50011, USA
[c] Department of Mechanical and Aerospace Engineering, University of Florida, Gainesville, FL 32611-6250, USA
[d] School of Materials Science and Engineering, Georgia Institute of Technology, Atlanta, GA 30332-0245, USA

ARTICLE INFO

Article history:
Received 8 April 2016
Received in revised form 19 June 2016
Accepted 19 June 2016
Available online xxxx

Keywords:
Concurrent atomistic-continuum method
Aluminum
Dislocation theory
Plastic deformation
Simulation

ABSTRACT

The bowing of edge dislocations from a row of collinear obstacles in Al is studied using concurrent atomistic-continuum simulations of submicron-sized realizations containing up to 238 million atoms. Results show that (1) as the number of adjacent bowed-out dislocation segments increases, the critical dislocation depinning stress approaches that for an infinite array of obstacles and (2) for the unstable overall semi-elliptic dislocation configuration, the presence of intermediate obstacles reduces the dislocation half-loop height, but doesn't affect the critical shear stress. Our work highlights the significance of the effects of adjacent bowed-out segments on cooperative dislocation bow-out.

Dislocation bow-out between pinning points is central to dislocation/obstacle interactions in crystalline materials [1]. Investigating the detailed process of dislocations bowing out and moving through a field of obstacles in metals aids in understanding the onset of flow through lattice, work hardening, and dislocation multiplication from Frank-Read sources [2]. Several modeling techniques, including molecular dynamics (MD) [3,4], dislocation dynamics (DD) [5,6], phase field method [7,8], and level set method [9], have been employed to simulate dislocation bow-out. In most of these studies, only one dislocation segment bows out from an isolated pair of obstacles. In reality, obstacles are distributed randomly in pure metals and alloys, with an average spacing L of about 30–300 nm [10,11]. Therefore, it is important to account for the effects of distributed bowed-out segments in modeling a given dislocation bow-out, in a way that considers both medium and long range elastic interactions as well as dislocation core effects.

Traditional dislocation bow-out analysis is based on dislocation line tension theory. Continuum dislocation theory predicts that the effective line tension of a curved dislocation segment is a logarithmic function of its initial distance L between two neighboring obstacles, namely, $\ln L$ [12]. In the presence of adjacent dislocation segments, however, the line tension of a given dislocation segment is altered [13]. Specifically, the negative interaction energy of a dislocation and its adjacent bowed-out segments reduces its line tension and hence lowers the critical stress required to bypass the obstacles [14]. This effect is particularly important for a dislocation line lying in a single slip plane and pinned by regularly spaced obstacles [14]. Simulations based on the dislocation self-stress show that, because of their opposite Burgers vector, the dipole-like attractive force between dislocation branches terminating on a given obstacle results in a "pinching" effect and facilitates dislocation bow-out [15,16]. The role of adjacent dislocation segments becomes more important with a decreasing D/L, where D is the obstacle diameter [17]. In dislocation/obstacle interactions, dislocations that depin from adjacent obstacles aid in pulling the branches together and diminish the strengthening effect [18].

Continuum models for dislocation/obstacle interactions apply to the dislocation bow-out process if the dislocation bypasses the obstacles following the Orowan bypass mechanism [19]. Most of these models assume that an infinitely long dislocation bypasses an infinite array of equally spaced obstacles. For obstacles with a finite size D, the term $\ln L$ is replaced by $\ln \overline{D}$ by taking into account of the interactions between three closest dislocation branches, where $\overline{D} = (D^{-1} + L^{-1})^{-1}$ [17]. Most simulations employ periodic boundary conditions (PBCs) along the dislocation line direction. In dislocation/precipitate interactions, Bacon et al. [17] included three precipitates in one simulation supercell with PBCs to represent an infinite row. Crone et al. [20] found that introducing additional voids beyond three doesn't show a significant influence on the critical depinning stress in dislocation/void interactions. Studies of a dislocation passing a random array of obstacles have been pursued using line tension models [21–23] and DD

* Corresponding author.
E-mail address: shuozhixu@gatech.edu (S. Xu).

http://dx.doi.org/10.1016/j.scriptamat.2016.06.018
1359-6462/

simulations [24]. Nevertheless, the effects of bow-out of other dislocation segments on the critical shear stress of a given dislocation bow-out in an image-free model have not been explored quantitatively, to the best of our knowledge.

In this paper, we perform quasistatic concurrent atomistic-continuum (CAC) simulations in the quasistatic, athermal limit to investigate edge dislocations bowing-out from a row of collinear cylindrical holes. A CAC simulation model, in general, contains an atomistic domain and a coarse-grained domain, in both of which the nucleation and propagation of dislocations and intrinsic stacking faults are permitted with a unified atomistic-continuum integral formulation [25]. In the coarse-grained domain, dislocations can pass between discontinuous elements [26]. Within each element, a finite element method with Gaussian quadrature is used to calculate the force/energy of the integration points and update the nodal positions, from which the positions of atoms inside the element are interpolated [27]. The coarse-grained description yields an accurate generalized stacking fault energy (GSFE) surface because the non-linear dislocation core structure/energy and Burgers vector are naturally accommodated [28].

Previously, CAC was applied to model nucleation and growth of dislocation loops in Cu, Al, and Si [29], dislocation-void interactions [30] in Ni, and dislocation-grain boundary interactions in Cu and Al [31]. The success of these calculations suggests the viability of using the CAC method to simulate cooperative dislocation bow-out in a sufficiently large model. Focus is placed on the critical shear stress and critical dislocation bow-out configuration — two important characteristics of the dislocation bow-out process. Face-centered cubic (FCC) Al is chosen because of its high stable SFE ($\approx$146 mJ/m^2) and low elastic anisotropy index ($\approx$1.21) [32], which enables the simulation results to be compared with most isotropic continuum models that don't consider dislocation dissociation. The embedded-atom method (EAM) potential of Mishin et al. [33] is adopted because the evaluated GSFE is close to the experimentally measured value [34]. The post-processing follows our earlier work [28,31], where more details of the CAC approach are given. Some runs are completed using Comet and Bridges on the NSF Extreme Science and Engineering Discovery Environment (XSEDE) [35].

Fig. 1(a) presents the simulation cell containing a row of 6 collinear cylindrical holes throughout the specimen along the z direction, which would potentially accommodate 5 dislocation segments between them. Full atomistic resolution is applied in the vicinity of holes such that the hole surface is at least 2 nm from the atomistic/coarse-grained interface; away from the holes, 3D rhombohedral discontinuous elements with surfaces corresponding to {111} slip planes are employed [26]. Within each second nearest neighbor element, piecewise continuous first order shape and interpolation functions are used; between elements, neither displacement continuity nor interelement compatibility is required [28]. The lattice orientations are $x[\bar{1}1\bar{2}]$, $y[110]$, and $z[1\bar{1}\bar{1}]$. With the lattice parameter $a_0 = 4.05$ Å, the simulation cell has a size of 300.59 nm by 297.22 nm by 45.49 nm; in all simulations, a uniform hole cross-sectional diameter on the x-y plane $D =$ 2.81 nm is used. With a constant interhole ligament distance $L =$ 5.61 nm, the number of initial dislocation segments n varies from 1 to 14, corresponding to a total ligament distance $L' = nL + (n-1)D$ between the leftmost and rightmost holes of 5.61–115.07 nm. As a result, the model with only one dislocation segment of L has 108,163 elements and 1,200,322 atoms, with 2,065,626 degrees of freedom in total, compared with 238,834,433 atoms in an equivalent full atomistic model, which would be highly computationally intensive. Simulations containing only two holes distanced by L' are also performed for comparison purposes, as shown in Fig. 1(b). All boundaries of the simulation cell as well as the hole surfaces are traction free such that the spurious forces arising from periodic images are eliminated [36]. The image forces on the bow-out from all boundaries can be estimated as follows:

1. In computing the image forces, the image dislocations can be assumed straight [36].
2. The image stresses arising from the surfaces normal to the x axis are stresses of a finite straight dislocation segment. Since the dislocation bow-out is collinear with but not on the image dislocations, the image stresses are zero according to Brown's formula [37].
3. The net image shear stress on the dislocation bow-out from the image dislocations of the two surfaces normal to the y axis is [12]

$$\tau_{zy}^{\text{image}} = \frac{\mu b}{4\pi(1-\nu)}\left|\frac{1}{l_y^+} - \frac{1}{l_y^-}\right| \tag{1}$$

where μ is the shear modulus, b is the magnitude of the Burgers vector of the full dislocation $b = (a_0/2)[110]$, ν is the Poisson's ratio, l_y^+ and l_y^- are the distances between the center-of-mass of the bowed dislocation and the surface whose outward normal vector is along the positive y and negative y directions, respectively. Initially, $l_y^+ = l_y^- = L_y/2$ where L_y is the length of the simulation cell along the y axis; hence, $\tau_{zy}^{\text{image}} = 0$. In the extreme case, the dislocations bow out to a semi-elliptic shape such that the center-of-mass of the bowed dislocation is moved by $4L/(3\pi)$ from its initial position, resulting in $l_y^+ = 148.61 - 4L/(3\pi) = 146.23$ nm and $l_y^- = 148.61 + 4L/(3\pi) = 150.99$ nm. Substituting $\mu = 28$ GPa, $b = 0.286$ nm, and $\nu = 0.33$ into Eq. (1) yields $\tau_{zy}^{\text{image}} = 0.205$ MPa. Note that this net image shear stress promotes dislocation bow-out.

4. The image forces from the surfaces normal to the z axis don't have any components on the x–y plane, within which the dislocation bow-out takes place [12]. Indeed, the net image force is zero since the dislocations are equidistant from both surfaces.

Straight edge dislocations are introduced on the mid-plane normal to the z axis by moving atoms/nodes inside the green lines in Fig. 1 by b, followed by energy minimization. Subsequently, a homogeneous shear stress τ_{zy} is applied, with atoms in adjacent to the holes constrained within the x–y plane to exclude dislocation climb and cross-slip of screw segments; these processes don't accompany the dislocation bow-out under consideration here. We emphasize that in the initial configuration, no dislocation segments pre-exist beyond the leftmost and rightmost holes, unlike those for classical dislocation/obstacle interactions where an infinitely long dislocation and an infinite array of obstacles are introduced [38,39]. The

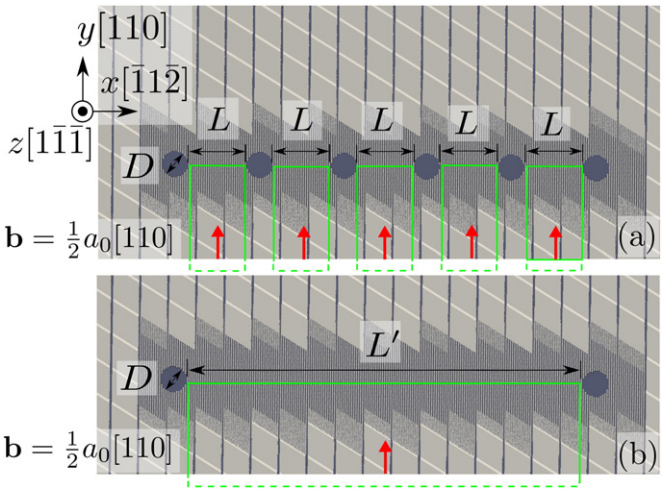

Fig. 1. CAC simulation cell containing (a) a row of 5 collinear initial dislocation segments each of which has a length of L and (b) one initial dislocation segment with length $L' = 5L + 4D$, where $L = 5.61$ nm and $D = 2.81$ nm. Cylindrical holes are throughout the specimen along the z direction. An atomistic domain is retained in the vicinity of the holes, while the coarse-grained domain is employed elsewhere. All boundaries are assumed stress free to alleviate spurious periodic image forces. Edge dislocations are formed by moving atoms/nodes inside the green lines by Burgers vector $b = (a_0/2)[110]$. (For interpretation of the references to colour in this figure legend, the reader is referred to the web version of this article.)